

Coexistence of pseudo-gap and charge order at the hot spots in cuprate superconductors

C. Pépin¹, V. S. de Carvalho^{1,2}, T. Kloss³ and X. Montiel³

¹*IPhT, L'Orme des Merisiers, CEA-Saclay, 91191 Gif-sur-Yvette, France*

²*Instituto de Física, Universidade Federal de Goiás, 74.001-970, Goiânia-GO, Brazil and*

³*International Institute of Physics, UFRN, Av. Odilon Gomes de Lima 1722, 59078-400 Natal, Brazil*

(Dated: August 25, 2014)

We address the timely issue of the presence of charge ordering at the hot-spots in the pseudo-gap phase of cuprate superconductors. Performing the Hubbard-Stratonovich decoupling such that the free energy stays always real and physically meaningful we exhibit three solutions of the spin-fermion model at the hot spots. A careful examination of their stability and free energy shows that, at low temperature, the system tends towards a co-existence of charge density wave and the composite order parameter made of diagonal quadrupolar density wave and pairing fluctuations of Ref. [Nat. Phys. **9**, 1745 (2013)]. The charge density wave is sensitive to the shape of the Fermi surface in contrast to the diagonal quadrupolar order, which is immune to it.

The discovery of charge order (CDW) in the Pseudo-Gap (PG) phase in non La-based Cuprate superconductors reached a steadily growing interest in recent years. Initially observed by STM in Bi2212 [1] and later in Bi2201 [2–8], the CDW phase was also observed in YBCO by quantum oscillation [9–13]. NMR [14–16] and Sound experiments [17, 18] confirmed the presence of CDW phase in YBCO while X-Ray bulk spectroscopy [19–25] has clearly characterized its checkerboard ordering with wave vector along the x and y axes $Q_x = Q_y = 0.33$ [26, 27]. Deeper analysis concluded that CDW ordering wave vector is located at the tips of the Fermi surface at the vicinity of the hot spots [25, 28, 29].

An additional phase transition to a checkerboard CDW ordered phase is observed at T_{CDW} [30] below the PG line at T^* [31, 32], $T_{CDW} < T^*$. Note that T^* coincides with the observation of loop current detected by neutron [33–37]. In temperature-doping phase diagram, the T_{CDW} -line has the typical form of a dome [38] and its magnitude is compound dependent [28, 29, 39, 40] whereas the PG-line is rather universal [39].

One of the most difficult challenge of the field is to understand how the recently observed CDW orders interferes with AF fluctuations and whether it participates or not to the formation of the PG phase. Although some alternative scenarios involving stronger Coulomb interactions have been considered [41–46], the proximity of the CDW ordering wave vector to the hot-spots is a strong incentive to consider the Spin-Fermion (SF) theory, which produced the most singular behavior at the hot-spots [47–49]. We follow here this route, keeping in mind that the SF model has been the subject of intense recent scrutiny [48, 50–57]. In particular, it has been shown that underlying SU(2) rotation exists between SC and charge sector which leaves the model invariant [50–52], producing a composite order parameter with a Quadrupolar d -wave component in the charge sector and preformed pairs in the SC sector (QDW/SC). This state of matter is a good candidate for the PG gap phase since it breaks translational symmetry and is thus able to produce a gap in the spectral functions. The ordering wave vector though lies on the diagonal while experiments report charge order at vectors \mathbf{Q}_x and \mathbf{Q}_y parallel to the axes of the compounds.

In this paper we introduce an original Hubbard-Stratonovich (HS) decoupling which enables us to consider the CDW order, and the QDW/SC order on the same footing. We find generically, that pure QDW/SC order is stable while the pure CDW is unstable. We show that at lower temperature a third solution emerges in which QDW/SC and CDW orders Co-Exist (CE solution). The transition towards coexistence is found to be weakly first order. Our conclusion is that the SF model supports the emergence of CDW with wave vectors parallel to the axes, but in coexistence with a larger instability, the QDW/SC order, which is a good candidate for the PG. The magnitude of the CDW order depends on the details of the Fermi surface topology while the QDW/SC order is insensitive to the shape of the Fermi surface.

Our starting point is the spin fermion model which can be described through the Lagrangian $L = L_\psi + L_\phi$ where

$$L_\psi = \psi^* (\partial_\tau + \epsilon_k + g\phi\sigma) \psi, \quad (1a)$$

$$L_\phi = \frac{1}{2} \phi D^{-1} \phi + \frac{u}{2} (\phi^2)^2. \quad (1b)$$

L_ψ is the fermion Lagrangian representing electrons with dispersion ϵ_k that are interacting with a bosonic spin excitation ϕ following Lagrangian L_ϕ . The spin-wave boson ϕ propagates through $D^{-1}(\omega, \mathbf{q}) = \frac{\omega^2}{v_s^2} + (\mathbf{q} - \mathbf{Q})^2 + m_a$, where v_s is the spin-wave velocity, \mathbf{Q} is the AF ordering wave vector, and m_a is the spin-wave boson mass, which vanishes at the QCP. We further simplify the problem by restricting the fermion dispersion represented in Fig. 1 to the eight hot spots, which are the only points with critical scattering through the paramagnons at $T = 0$.

The Fermi velocity is further linearized and written into the matrix form $\hat{\epsilon}_k = v_x \hat{x} + v_y \hat{y}$, with $\hat{x} = (k_x P_{\Sigma_x} - k_y P_{\Sigma_y}) \Lambda_3 L_3$, $\hat{y} = (k_y P_{\Sigma_x} - k_x P_{\Sigma_y}) \Lambda_3$, $v_x = v \cos \theta$, $v_y = v \sin \theta$, with θ the angle of the Fermi velocity with the x -axis. Λ_3 and L_3 are Pauli matrices of the 16×16 symmetry space $(\Sigma, \Lambda, L, \tau)$. Here the first three tensor products (Σ, Λ, L) describe the symmetries of the Brillouin Zone (BZ), with respectively Σ for the permutation of two hot spots inside a pair of hot spots, Λ the permutation of two pairs of hot spots inside a quartet and L for the permutation of the two quartets of hot spots, while

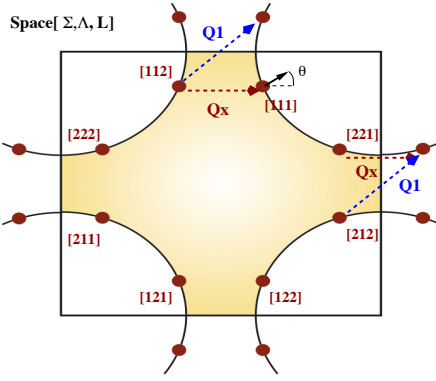


FIG. 1. (Color online) Schematic Fermi surface of cuprate superconductors in the first Brillouin zone of a square lattice. The eight hot spots are depicted with red dots labeled with the (Σ, Λ, L) -space. The angle θ is defined between the velocity vector at the $[111]$ -hotspot with the x -axis. The experimentally observed CDW wave vector \mathbf{Q}_x connects the L_2 -sector, whereas the diagonal QDW/SC vector \mathbf{Q}_1 does not.

τ stands for the particle-hole space. $P_{\Sigma_x} = (1 + \Sigma_3)/2$ and $P_{\Sigma_y} = (1 - \Sigma_3)/2$ are projection operators onto the first and second component of the Σ -space.

The spin-boson field ϕ is then formally integrated out of the partition function to get the following effective partition function $Z = \int d\psi \exp(-S_0 - S_{int})$ with (here $x = (\mathbf{r}, \tau)$ and the trace Tr is taken over the 16×16 matrix space)

$$S_0 = \int dx dx' \bar{\psi}_x g_0^{-1} \psi_{x'}, \quad (2a)$$

$$S_{int} = \frac{3g^2}{2} \int dx dx' \text{Tr} (D_{x-x'} \psi_x \bar{\psi}_{x'} \Sigma_1 \psi_{x'} \psi_x \Sigma_1). \quad (2b)$$

There are many ways to decouple the action of Eq. (2) into the physically relevant hydro-dynamic modes of the system. The issue we face here is that the various order parameters that we want to study simultaneously have different symmetries. On one hand the candidate for the PG phase, the QDW/SC order parameter writes [52] $\hat{B}_1 = B_1(\epsilon_n, \mathbf{q}) \hat{U}$, with $\hat{U}_\Lambda = i \begin{pmatrix} 0 & \hat{u}_\tau \\ -\hat{u}_\tau^\dagger & 0 \end{pmatrix}_\Lambda$, $\hat{u}_\tau = \begin{pmatrix} \Delta_- & \Delta_+ \\ -\Delta_+^* & \Delta_-^* \end{pmatrix}_\tau$. Herein $\Delta_- = \sum_{\mathbf{k}} \langle \psi_{\mathbf{k}}^\dagger \psi_{\mathbf{k}+\mathbf{Q}_{1,2}} \rangle$ is the QDW component, with $\mathbf{Q}_{1,2} = (\mathbf{Q}_x \pm \mathbf{Q}_y)/2$, the diagonal vector. $\Delta_+ = \langle \psi_{\mathbf{k},\sigma} \psi_{-\mathbf{k},-\sigma} \rangle$ is the d -wave SC component. On the other hand, any CDW with wave vector parallel to the x, y -axes must involve some off-diagonal component in the L -sector. Here we work with $\hat{B}_2 = \begin{pmatrix} B_{2x} & 0 \\ 0 & B_{2y} \end{pmatrix}_\Sigma L_2 \otimes \Lambda_3$. Note that this choice produces a ‘‘stripe’’ type of order parameter with vectors parallel to \mathbf{Q}_x . We defer a detailed study of the nematicity to a later work. In the form of the order parameter \hat{B}_2 , different amplitudes are allowed in the P_{Σ_x} and P_{Σ_y} sectors, which corresponds to a mixture of s - and d -wave symmetry around the Fermi surface[58]. When solving self-consistently for \hat{B}_1 and \hat{B}_2 , the same s - d anisotropy must be tolerated for \hat{B}_1 leading to

$$\hat{B}_1 = \begin{pmatrix} B_{1x} & 0 \\ 0 & B_{1y} \end{pmatrix}_\Sigma \hat{U}_\Lambda.$$

The most generic HS decoupling can be written (herein $\tilde{\gamma}^{-1} = \frac{2}{3g^2} D^{-1}$)

$$Z = \frac{\int \mathcal{D}[\psi] \mathcal{D}[Q_a, Q_b] I[Q_a, Q_b, \psi] \exp[-S_0 - S_{int}]}{\int \mathcal{D}[Q_a, Q_b] I[Q_a, Q_b, 0]}, \quad (3a)$$

$$I[Q_a, Q_b, \psi] = \exp[-\tilde{\gamma}^{-1} (Q_a - i\tilde{\gamma}\psi_x \bar{\psi}_{x'}) (Q_b - i\tilde{\gamma}\Sigma_1 \psi_{x'} \bar{\psi}_x \Sigma_1)]. \quad (3b)$$

In Eq. (3a) we must ensure that the quadratic form in the exponential is always positive definite and that the resulting free energy is real for any field $Q_{a,b}$. We choose $Q_a = \Sigma_1 Q^\dagger \Sigma_1$ and $Q_b = Q$. This relation defines a new charge conjugation

$$\bar{Q} = \Sigma_1 Q^\dagger \Sigma_1, \quad (4)$$

that will be used in the remainder of our study. Using Eq. (4) and setting $Q_{x,y} = i\hat{B}_{x,y}$, [resp. $\bar{Q}_{x,y} = -i\hat{B}_{y,x}$], the free energy becomes

$$F = F_0 + F_x + F_y, \quad (5a)$$

$$F_0 = T \sum_{\epsilon} \int \frac{d\mathbf{p}}{(2\pi)^2} \tilde{\gamma}^{-1} [\hat{B}_x \hat{B}_x + \hat{B}_y \hat{B}_y], \quad (5b)$$

$$F_{x(y)} = -\frac{1}{2} T \sum_{\epsilon} \int \frac{d\mathbf{p}}{(2\pi)^2} \text{Tr} \ln (g_{0x(y)}^{-1} - \hat{b}_{1x(y)} - \hat{b}_{2x(y)}), \quad (5c)$$

with $g_{0x}^{-1} = i\epsilon - \hat{x}_{\mathbf{p}}$, $\hat{x}_{\mathbf{p}} = vp_x \cos \theta \Lambda_3 L_3 + vp_y \sin \theta \Lambda_3$, $g_{0y}^{-1} = i\epsilon - \hat{y}_{\mathbf{p}}$, $\hat{y}_{\mathbf{p}} = -vp_x \sin \theta \Lambda_3 L_3 - vp_y \cos \theta \Lambda_3$, $\hat{b}_x = \hat{B}_x + \hat{B}_y$ and $\hat{b}_y = \hat{B}_y + \hat{B}_x$. Using $\text{Tr} \ln G^{-1} = \ln \det G^{-1}$, where $G^{-1} = g_{0x(y)}^{-1} - \hat{b}_{1x(y)} - \hat{b}_{2x(y)}$, we can write the free energy involving only scalar functions as

$$F_0 = T \sum_{\epsilon} \int \frac{d\mathbf{p}}{(2\pi)^2} \tilde{\gamma}^{-1} [\bar{B}_{1x} B_{1x} + \bar{B}_{1y} B_{1y} + \bar{B}_{2x} B_{2x} + \bar{B}_{2y} B_{2y}], \quad (6a)$$

$$F_x = -\frac{1}{2} T \sum_{\epsilon} \int \frac{d\mathbf{p}}{(2\pi)^2} [-\ln(d_x - b_{2x}^2) + \ln((\epsilon^2 + b_{1x}^2) d_x^2 + (vp_x \cos \theta d_x + vp_y \sin \theta (d_x - 2b_{2x}^2))^2)], \quad (6b)$$

$$F_y = -\frac{1}{2} T \sum_{\epsilon} \int \frac{d\mathbf{p}}{(2\pi)^2} [-\ln(d_y - b_{2y}^2) + \ln((\epsilon^2 + b_{1y}^2) d_y^2 + (vp_x \sin \theta d_y + vp_y \cos \theta (d_y - 2b_{2y}^2))^2)], \quad (6c)$$

$$d_x = \epsilon^2 + (vp_x \cos \theta - vp_y \sin \theta)^2 + b_{1x}^2 + b_{2x}^2,$$

$$d_y = \epsilon^2 + (vp_x \sin \theta - vp_y \cos \theta)^2 + b_{1y}^2 + b_{2y}^2.$$

Eqs. (6) and the introduction of the new conjugation Eq. (4) constitute the main technical tools of this paper which enable a controlled discussion of the co-existence and interplay of the two order parameters \hat{B}_1 (QDW/SC) and \hat{B}_2 (CDW).

The Mean-Field Equations (MFEs) are derived by differentiation of the free energy Eq. (5) with respect to $\bar{B}_{x,y}$ and $B_{x,y}$ successively. Notably, when imposing the constraint $\bar{B}_x = B_y$

and $\bar{B}_y = B_x$ after differentiation, the MFEs reduce to four independent equations. This reduction reflects the original symmetry of the system and is a check that the correct conjugation relation was introduced. The MFEs write

$$B_{1x}(\varepsilon_n) = 4\gamma_0 T \sum_{\varepsilon'} A_{1x}(\varepsilon_n, \varepsilon'_n) B_{1y}(\varepsilon'_n), \quad (7a)$$

$$B_{1y}(\varepsilon_n) = 4\gamma_0 T \sum_{\varepsilon'} A_{1y}(\varepsilon_n, \varepsilon'_n) B_{1x}(\varepsilon'_n), \quad (7b)$$

$$B_{2x}(\varepsilon_n) = 4\gamma_1 T \sum_{\varepsilon'} A_{2x}(\varepsilon_n, \varepsilon'_n) B_{2y}(\varepsilon'_n), \quad (7c)$$

$$B_{2y}(\varepsilon_n) = 4\gamma_1 T \sum_{\varepsilon'} A_{2y}(\varepsilon_n, \varepsilon'_n) B_{2x}(\varepsilon'_n), \quad (7d)$$

where $\gamma_0 = 3g^2/2$, $\gamma_1 = 3g_1^2/2$ and the parameters $A_{i,x}$, $A_{i,y}$ are given by

$$A_{1x} = \sum_{\mathbf{q}} \frac{D_{\omega, \mathbf{q}}}{V} \left(\frac{d_x + 2vq_x vq_y \cos \theta \sin \theta}{d_x^2 + 4vq_x vq_y \cos \theta \sin \theta d_x - 4b_{2x}^2 v^2 q_y^2 \sin^2 \theta} \right), \quad (8a)$$

$$A_{2x} = \sum_{\mathbf{q}} \frac{D_{\omega, \mathbf{q}}}{V} \left(\frac{d_x + 2vq_x vq_y \cos \theta \sin \theta - 2v^2 q_y^2 \sin^2 \theta}{d_x^2 + 4vq_x vq_y \cos \theta \sin \theta d_x - 4b_{2x}^2 v^2 q_y^2 \sin^2 \theta} \right), \quad (8b)$$

$$A_{1y} = \sum_{\mathbf{q}} \frac{D_{\omega, \mathbf{q}}}{V} \left(\frac{d_y + 2vq_x vq_y \cos \theta \sin \theta}{d_y^2 + 4vq_x vq_y \cos \theta \sin \theta d_y - 4b_{2y}^2 v^2 q_x^2 \cos^2 \theta} \right), \quad (8c)$$

$$A_{2y} = \sum_{\mathbf{q}} \frac{D_{\omega, \mathbf{q}}}{V} \left(\frac{d_y + 2vq_x vq_y \cos \theta \sin \theta - 2v^2 q_x^2 \cos^2 \theta}{d_y^2 + 4vq_x vq_y \cos \theta \sin \theta d_y - 4b_{2y}^2 v^2 q_x^2 \cos^2 \theta} \right), \quad (8d)$$

$$\text{with } D_{\omega, \mathbf{q}} = (\gamma|\omega| + q_x^2 + q_y^2 + a),$$

where $\frac{1}{V} \sum_{\mathbf{q}} \equiv \int \frac{d\mathbf{q}}{(2\pi)^2}$. A closer look at Eq. (8) shows that the right hand-side of (7a) and (7d) is always lower than the r.h.s. of resp. (7b) and (7c). In order for the two solutions to exist simultaneously, it is enough to introduce a slightly different coefficient γ_1 in front of (7b) and (7d), with $g_1 \geq g$, which henceforth will favor the B_2 -type of decoupling. This difference can be introduced through a small additional interaction. Such an interaction will be generated for instance by correlations of the form $u\rho_{\mathbf{Q}_x}\rho_{-\mathbf{Q}_x}\langle\rho_{\mathbf{Q}_y}\rho_{-\mathbf{Q}_y}\rangle$ which are breaking orthorhombic symmetry.

The typical result of the MFEs for parameters $g_1 \simeq g$ is given in Fig. 2. We observe that three solutions are obtained, i) the pure QDW/SC solution for which $B_1 \neq 0$ and $B_2 = 0$; ii) the pure CDW solution for which $B_2 \neq 0$ and $B_1 = 0$; iii) the Co-Existence (CE) solution where $B_1 \neq 0$ and $B_2 \neq 0$. Moreover, for typical values of the coupling constants, solution i) and ii) have similar magnitude, while for the CE solution $B_2 \ll B_1$. The dependence on the Fermi velocity angle θ which captures the dependence of the solutions on the fermiology of the compounds is depicted in Fig. 3. We find that the pure QDW/SC solution i) is insensitive to fermiology, whereas the pure CDW solution ii) is more favorable when

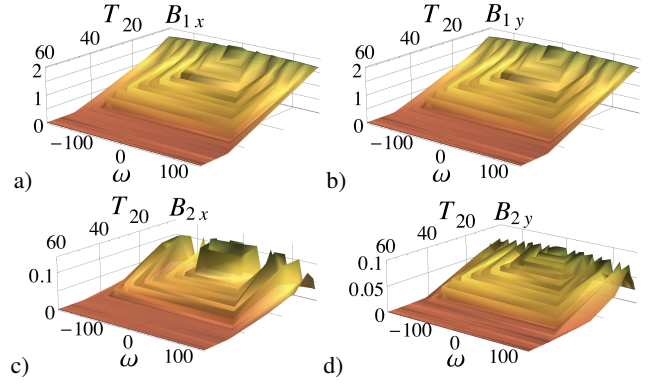


FIG. 2. (Color online) Typical form of the order parameters in the CE phase as a function of frequency ω and temperature T : $B_{1x/1y}$ (depicted in panel a) and b)) representing QDW/SC and $B_{2x/2y}$ (depicted in panel c) and d)) representing CDW order. Note that the CDW component is one order of magnitude smaller than the QDW/SC solution. We take g_1 slightly bigger than g in order to stabilize the CDW sector. The actual figure corresponds to $g = 20$, $g_1 = 30$, $v = 6$, $m_a = 0.1$, $\gamma = 3$, $W = 2\pi$ and $\theta = 0.1$.

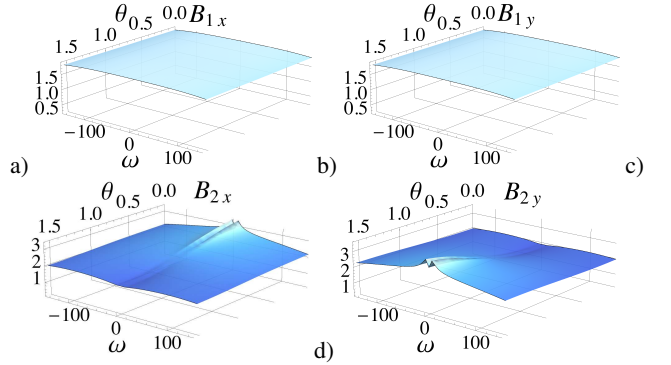


FIG. 3. (Color online) Typical form of the order parameters in the CE phase as a function of frequency ω and velocity angle θ : $B_{1x/1y}$ (depicted in panel a) and b)) representing QDW/SC and $B_{2x/2y}$ (depicted in panel c) and d)) representing CDW order. Note that the CDW component is one order of magnitude smaller than the QDW/SC solution. The parameters are the same as in Fig. 2.

$\theta = 0$, which correspond to flat portions of the Fermi surface in the anti-nodal region. The insensitivity of the QDW/SC solution to the value of θ stems from the fact that, in our matrix framework $\{\hat{B}_1, \hat{\varepsilon}_k\} = 0$, which is not the case for the CDW order.

We turn now to the Gaussian fluctuations. We expand Eq. (6) to the second order in the fluctuation field δB_{1x} , δB_{1y} , δB_{2x} , δB_{2y} and their conjugate. We find

$$\Delta F = \frac{T}{V} \sum_{\varepsilon} \sum_{\mathbf{k}, \mathbf{k}'} \sum_{i=1}^2 \left[\gamma_{\mathbf{k}-\mathbf{k}'}^{-1} \delta \bar{B}_{i,\mathbf{k}} \delta B_{i,\mathbf{k}'} - \left(\frac{A_{i,\mathbf{k}} - \delta A_{i,\mathbf{k}}}{4} \right) \delta b_{i,\mathbf{k}}^2 \delta_{\mathbf{k}, \mathbf{k}'} \right], \quad (9)$$

with $\delta b_{i,\mathbf{k}} = \delta \bar{B}_{i,\mathbf{k}} + \delta B_{i,\mathbf{k}}$. In order to study the stability of the various solution, we write the quadratic form $\Delta F = \frac{1}{2} \sum_{i=1}^2 \Psi_i^\dagger M_i \Psi_i$, with $\Psi_i = (\delta B_{i,x}, \delta \bar{B}_{i,y}, \delta \bar{B}_{i,x}, \delta B_{i,y})^T$ and $\Psi_i^\dagger =$

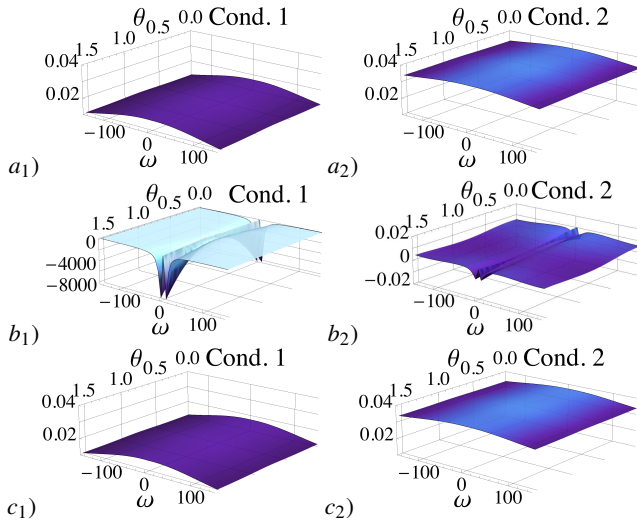


FIG. 4. (Color online) Stability conditions (l.h.s. of Eq. (11)) as a function of frequency ω and velocity angle θ for the three possible solutions in the directions of B_1 and B_2 : Pure QDW/SC for a_1 [dir. B_1] and a_2 [dir. B_2]; pure CDW solution for b_1 [dir. B_1] and b_2 [dir. B_2] and CE solution for c_1) and c_2). Note that the pure CDW solution is always unstable while the CE solution is stable. The parameters are the same as in Fig. 3.

$(\delta B_{ix}, \delta \bar{B}_{iy}, \delta \bar{B}_{ix}, \delta B_{iy})$. The matrix M writes

$$M = \begin{pmatrix} \gamma^{-1} & 0 & \bar{A}_x & \bar{A}_x \\ 0 & \gamma^{-1} & \bar{A}_x & \bar{A}_x \\ \bar{A}_y & \bar{A}_y & \gamma^{-1} & 0 \\ \bar{A}_y & \bar{A}_y & 0 & \gamma^{-1} \end{pmatrix}, \quad (10)$$

with $\bar{A}_x = (A_x - \delta A_x)/2$ and $\bar{A}_y = (A_y - \delta A_y)/2$. The stability condition corresponds to the condition for which M is positive definite. One can convince oneself that this condition is equivalent to $\det M \geq 0$, which leads to

$$\gamma^{-2} - 4\bar{A}_x\bar{A}_y \geq 0. \quad (11)$$

Note that the free energy (9) is always real. When $\delta A_x = 0$, Eq. (11) is equivalent to the condition for existence of MF solutions [Eqs. (7)]. The stability condition in the respective directions $B_{1x(y)}$ and $B_{2x(y)}$ are presented in Fig. 4. Typically, one observes that the pure QDW/SC solution is stable [Fig. 4, a_1) and a_2)] while the pure CDW solution is unstable [Fig. 4, b_1) and b_2)]. The CE solution is always stable at low temperatures [Fig. 4, c_1) and c_2)].

In order to differentiate between the two stable solutions [pure QDW/SC and CE] we evaluate the free energy in Fig. 5. We see that the CE solution is slightly lower than the pure QDW/SC solution. This behavior is also observed in the limit $\gamma_1 \gg \gamma_0$. Our conclusion is that the generic tendency is a transition of slightly first order towards the CE solution at lower temperatures.

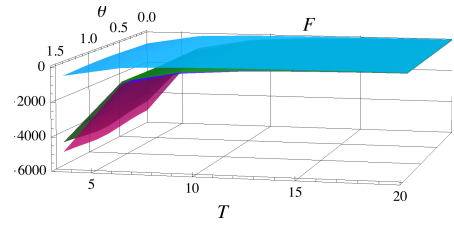


FIG. 5. (Color online) Free energy F of the three MF solutions as a function of θ and T : pure CDW (blue), pure QDW/SC (green) and CE (magenta). Note that the free energy for the CE solution is slightly lower than for both the QDW/SC and the CDW solutions. The parameters are the same as in Fig. 2

Simple Hartree-Fock evaluations generically produces charge ordering wave vectors on the diagonal at $(\mathbf{Q}_x \pm \mathbf{Q}_y)/2$ [53, 59] and similarly with the solution of the gap equation for the QDW/SC solution [52, 60], whereas nothing is observed on the diagonal. To resolve this discrepancy, some works have introduced Coulomb interactions [44, 45], but the wave vector is still a bit tilted. Another interesting proposal is to use the three bands model and evaluate the charge response on top of an anti-ferromagnetic PG [46]. We have also suggested to use SC fluctuation to stabilize CDW with correct wave vector at the anti-nodes[61]. Lately, a closely related work to ours has suggested that CDW occurs directly at the hot spots[54]. Our findings agree with Ref.[54] in the understanding that a competition exists at the hot spots between the CDW and the QDW/SC. However, we find that even when the coupling constants are tuned so that the CDW ordering is extremely favorable, at lower temperature the QDW/SC re-emerges to form a CE solution.

Our conclusion is that CDW order can be stabilized at the hot spots of the SF model in co-existence with the QDW/SC solution. The CDW can be considered as a bi-product of the emergence of the QDW/SC order. Its magnitude is picked at T_c and non-linear σ -models uniting QDW and SC [52, 56, 60] to explain sound experiments and X-rays findings are still valid.

We are grateful for discussions with O. Babelon concerning the HS transformation and reduction of the free energy. Discussions with M. Eienkel, H. Meier, K. Efetov and A. Chubukov are also acknowledged. C.P. acknowledges the support from the grant EXCELCIUS of the Labex PALM of the Université Paris-Saclay, and the project UNESCOS of the ANR. V.S. de C. acknowledges the support of CAPES and X.M. and T.K. founding from the IIP.

-
- [1] J. E. Hoffman, E. W. Hudson, K. M. Lang, V. Madhavan, H. Eisaki, S. Uchida, and J. C. Davis, *Science* **295**, 466 (2002).
 - [2] T. Hanaguri, C. Lupien, Y. Kohsaka, D. H. Lee, M. Azuma, M. Takano, H. Takagi, and J. C. Davis, *Nature* **430**, 1001 (2004).
 - [3] K. McElroy, D.-H. Lee, J. E. Hoffman, K. M. Lang, J. Lee, E. W. Hudson, H. Eisaki, S. Uchida, and J. C. Davis, *Phys. Rev. Lett.* **94**, 197005 (2005).

- [4] K. McElroy, G.-H. Gweon, S. Y. Zhou, J. Graf, S. Uchida, H. Eisaki, H. Takagi, T. Sasagawa, D.-H. Lee, and A. Lanzara, *Phys. Rev. Lett.* **96**, 067005 (2006).
- [5] Y. Kohsaka, C. Taylor, K. Fujita, A. Schmidt, C. Lupien, T. Hanaguri, M. Azuma, M. Takano, H. Eisaki, H. Takagi, S. Uchida, and J. C. Davis, *Science* **315**, 1380 (2007).
- [6] W. D. Wise, M. C. Boyer, K. Chatterjee, T. Kondo, T. Takeuchi, H. Ikuta, Y. Wang, and E. W. Hudson, *Nat. Phys.* **4**, 696 (2008).
- [7] Y. He, a. Yi Yin, M. Zech, A. Soumyanarayanan, M. M. Yee, T. Williams, b. M C Boyer, K. Chatterjee, W. D. Wise, I. Zeljkovic, c. T. T. Takeshi Kondo, H. Ikuta, P. Mistark, R. S. Markiewicz, A. Bansil, S. Sachdev, d. E W Hudson, and J E Hoffman, *Science* **344**, 608 (2014).
- [8] E. H. da Silva Neto, P. Aynajian, A. Frano, R. Comin, E. Schierle, E. Weschke, A. Gyenis, J. Wen, J. Schneeloch, Z. Xu, S. Ono, G. Gu, M. Le Tacon, and A. Yazdani, *Science* **343**, 393 (2014).
- [9] N. Doiron-Leyraud, C. Proust, D. LeBoeuf, J. Levallois, J.-B. Bonnemaison, R. Liang, D. A. Bonn, W. N. Hardy, and L. Taillefer, *Nature* **447**, 565 (2007).
- [10] D. LeBoeuf, N. Doiron-Leyraud, J. Levallois, R. Daou, J. B. Bonnemaison, N. E. Hussey, L. Balicas, B. J. Ramshaw, R. Liang, D. A. Bonn, W. N. Hardy, S. Adachi, C. Proust, and L. Taillefer, *Nature* **450**, 533 (2007).
- [11] S. E. Sebastian, N. Harrison, M. M. Altarawneh, C. H. Mielke, R. Liang, D. A. Bonn, and G. G. Lonzarich, *PNAS* **107**, 6175 (2010).
- [12] F. Laliberté, J. Chang, N. Doiron-Leyraud, E. Hassinger, R. Daou, M. Rondeau, B. J. Ramshaw, R. Liang, D. A. Bonn, W. N. Hardy, S. Pyon, T. Takayama, H. Takagi, I. Sheikin, L. Malone, C. Proust, K. Behnia, and L. Taillefer, *Nat. Commun.* **2**, 432 (2011).
- [13] S. E. Sebastian, N. Harrison, R. Liang, D. A. Bonn, W. N. Hardy, C. H. Mielke, and G. G. Lonzarich, *Phys. Rev. Lett.* **108**, 196403 (2012).
- [14] T. Wu, H. Mayaffre, S. Krämer, M. Horvatic, C. Berthier, W. N. Hardy, R. Liang, D. A. Bonn, and M.-H. Julien, *Nature* **477**, 191 (2011).
- [15] T. Wu, H. Mayaffre, S. Krämer, M. Horvatić, C. Berthier, P. L. Kuhns, A. P. Reyes, R. Liang, W. N. Hardy, D. A. Bonn, and M.-H. Julien, *Nat. Commun.* **4** (2013).
- [16] T. Wu, H. Mayaffre, S. Krämer, M. Horvatić, C. Berthier, W. N. Hardy, R. Liang, D. A. Bonn, and M.-H. Julien, *arXiv:cond-mat/1404.1617* (2014).
- [17] D. LeBoeuf, S. Kramer, W. N. Hardy, R. Liang, D. A. Bonn, and C. Proust, *Nat. Phys.* **9**, 79 (2013).
- [18] A. Shekhter, B. J. Ramshaw, R. Liang, W. N. Hardy, D. A. Bonn, F. F. Balakirev, R. D. McDonald, J. B. Betts, S. C. Riggs, and A. Migliori, *Nature* **498**, 75 (2013).
- [19] M. Le Tacon, G. Ghiringhelli, J. Chaloupka, M. M. Sala, V. Hinkov, M. W. Haverkort, M. Minola, M. Bakr, K. J. Zhou, S. Blanco-Canosa, C. Monney, Y. T. Song, G. L. Sun, C. T. Lin, G. M. De Luca, M. Salluzzo, G. Khaliullin, T. Schmitt, L. Braicovich, and B. Keimer, *Nat. Phys.* **7**, 725 (2011).
- [20] J. Chang, E. Blackburn, A. T. Holmes, N. B. Christensen, J. Larsen, J. Mesot, R. Liang, D. A. Bonn, W. N. Hardy, A. Watenphul, M. v. Zimmermann, E. M. Forgan, and S. M. Hayden, *Nat. Phys.* **8**, 871 (2012).
- [21] G. Ghiringhelli, M. Le Tacon, M. Minola, S. Blanco-Canosa, C. Mazzoli, N. B. Brookes, G. M. De Luca, A. Frano, D. G. Hawthorn, F. He, T. Loew, M. M. Sala, D. C. Peets, M. Salluzzo, E. Schierle, R. Sutarto, G. A. Sawatzky, E. Weschke, B. Keimer, and L. Braicovich, *Science* **337**, 821 (2012).
- [22] E. Blackburn, J. Chang, A. H. Said, B. M. Leu, R. Liang, D. A. Bonn, W. N. Hardy, E. M. Forgan, and S. M. Hayden, *Phys. Rev. B* **88**, 054506 (2013).
- [23] S. Blanco-Canosa, A. Frano, T. Loew, Y. Lu, J. Porras, G. Ghiringhelli, M. Minola, C. Mazzoli, L. Braicovich, E. Schierle, E. Weschke, M. Le Tacon, and B. Keimer, *Phys. Rev. Lett.* **110**, 187001 (2013).
- [24] M. Le Tacon, A. Bosak, S. M. Souliou, G. Dellea, T. Loew, R. Heid, K.-P. Bohnen, G. Ghiringhelli, M. Krisch, and B. Keimer, *Nat. Phys.* **10**, 52 (2014).
- [25] S. Blanco-Canosa, A. Frano, E. Schierle, J. Porras, T. Loew, M. Minola, M. Bluschke, E. Weschke, B. Keimer, and M. Le Tacon, *arXiv:cond-mat/1406.1595* (2014).
- [26] N. Harrison and S. E. Sebastian, *Phys. Rev. Lett.* **106**, 226402 (2011).
- [27] N. Harrison and S. E. Sebastian, *New J. Phys.* **16**, 063025 (2014).
- [28] I. M. Vishik, M. Hashimoto, R.-H. He, W.-S. Lee, F. Schmitt, D. Lu, R. G. Moore, C. Zhang, W. Meevasana, T. Sasagawa, S. Uchida, K. Fujita, S. Ishida, M. Ishikado, Y. Yoshida, H. Eisaki, Z. Hussain, T. P. Devereaux, and Z.-X. Shen, *PNAS* **109**, 18332 (2012).
- [29] R. Comin, A. Frano, M. M. Yee, Y. Yoshida, H. Eisaki, E. Schierle, E. Weschke, R. Sutarto, F. He, A. Soumyanarayanan, Y. He, M. Le Tacon, I. S. Elfimov, J. E. Hoffman, G. A. Sawatzky, B. Keimer, and A. Damascelli, *Science* **343**, 390 (2014).
- [30] J. Xia, E. Schemm, G. Deutscher, S. A. Kivelson, D. A. Bonn, W. N. Hardy, R. Liang, W. Siemons, G. Koster, M. M. Fejer, and A. Kapitulnik, *Phys. Rev. Lett.* **100**, 127002 (2008).
- [31] H. Alloul, T. Ohno, and P. Mendels, *Phys. Rev. Lett.* **63**, 1700 (1989).
- [32] W. W. Warren, R. E. Walstedt, G. F. Brenner, R. J. Cava, R. Tycko, R. F. Bell, and G. Dabbagh, *Phys. Rev. Lett.* **62**, 1193 (1989).
- [33] B. Fauqué, Y. Sidis, V. Hinkov, S. Pailhès, C. T. Lin, X. Chaud, and P. Bourges, *Phys. Rev. Lett.* **96**, 197001 (2006).
- [34] C. M. Varma, *Phys. Rev. B* **73**, 155113 (2006).
- [35] V. Balédent, D. Haug, Y. Sidis, V. Hinkov, C. T. Lin, and P. Bourges, *Phys. Rev. B* **83**, 104504 (2011).
- [36] P. Bourges and Y. Sidis, *Comptes Rendus Physique* **12**, 461 (2011).
- [37] Y. Sidis and P. Bourges, *J. Phys.: Conf. Ser.* **449**, 012012 (2013).
- [38] G. Grissonnanche, O. Cyr-Choinière, F. Laliberté, S. Renéde Cotret, A. Juneau-Fecteau, S. Dufour-Beauséjour, M. È. Delage, D. LeBoeuf, J. Chang, B. J. Ramshaw, D. A. Bonn, W. N. Hardy, R. Liang, S. Adachi, N. E. Hussey, B. Vignolle, C. Proust, M. Sutherland, S. Krämer, J. H. Park, D. Graf, N. Doiron-Leyraud, and L. Taillefer, *Nat. Commun.* **5** (2014).
- [39] H. Alloul, *Comptes Rendus Physique* **15**, 519 (2014).
- [40] W. Tabis, Y. Li, M. Le Tacon, L. Braicovich, A. Kreyssig, M. Minola, G. Dellea, E. Weschke, M. J. Veit, M. Ramazanoglu, A. I. Goldman, T. Schmitt, G. Ghiringhelli, N. Barišić, M. K. Chan, C. J. Dorow, G. Yu, X. Zhao, B. Keimer, and M. Greven, *arXiv:cond-mat/1404.7658* (2014).
- [41] S. Chakravarty, R. B. Laughlin, D. K. Morr, and C. Nayak, *Phys. Rev. B* **63**, 094503 (2001).
- [42] S. A. Kivelson, I. P. Bindloss, E. Fradkin, V. Oganesyan, J. M. Tranquada, A. Kapitulnik, and C. Howald, *Rev. Mod. Phys.* **75**, 1201 (2003).
- [43] E.-A. Kim, M. J. Lawler, P. Oreto, S. Sachdev, E. Fradkin, and S. A. Kivelson, *Phys. Rev. B* **77**, 184514 (2008).
- [44] A. Allais, J. Bauer, and S. Sachdev, *Indian J. Phys.* **88**, 905

- (2014).
- [45] A. Allais, J. Bauer, and S. Sachdev, [arXiv:cond-mat/1402.4807](#) (2014).
 - [46] W. A. Atkinson, A. P. Kampf, and S. Bulut, [arXiv.org](#) (2014).
 - [47] A. J. Millis and H. Monien, *Phys. Rev. Lett.* **70**, 2810 (1993).
 - [48] A. Abanov, A. V. Chubukov, and J. Schmalian, *Adv. Phys.* **52**, 119 (2003).
 - [49] A. Abanov and A. Chubukov, *Phys. Rev. Lett.* **93**, 255702 (2004).
 - [50] M. A. Metlitski and S. Sachdev, *New J. Phys.* **12**, 105007 (2010).
 - [51] M. A. Metlitski and S. Sachdev, *Phys. Rev. B* **82**, 075128 (2010).
 - [52] K. B. Efetov, H. Meier, and C. Pépin, *Nat. Phys.* **9**, 1745 (2013).
 - [53] S. Sachdev and R. La Placa, *Phys. Rev. Lett.* **111**, 027202 (2013).
 - [54] Y. Wang and A. Chubukov, *Phys. Rev. B* **90**, 035149 (2014).
 - [55] M. Eimenkel, H. Meier, C. Pépin, and K. B. Efetov, [arXiv:cond-mat/1407.5794](#) (2014).
 - [56] L. E. Hayward, D. G. Hawthorn, R. G. Melko, and S. Sachdev, *Science* **343**, 1336 (2014).
 - [57] D. Chowdhury and S. Sachdev, [arXiv:cond-mat/1404.6532](#) (2014).
 - [58] K. Fujita, C. K. Kim, I. Lee, J. Lee, M. Hamidian, I. A. Firmo, S. Mukhopadhyay, H. Eisaki, S. Uchida, M. J. Lawler, E. A. Kim, and J. C. Davis, *Science* **344**, 612 (2014).
 - [59] A. Allais, D. Chowdhury, and S. Sachdev, [arXiv:cond-mat/1406.0503](#) (2014).
 - [60] H. Meier, M. Eimenkel, C. Pépin, and K. B. Efetov, *Phys. Rev. B* **88**, 020506 (2013).
 - [61] H. Meier, C. Pépin, M. Eimenkel, and K. B. Efetov, *Phys. Rev. B* **89**, 195115 (2014).

Supplementary Information

I. REDUCTION OF THE FREE ENERGY

For further details about the notations, we refer the reader to the SI of our previous paper [52]. We give here the essential steps in the reduction of the free energy leading to Eq. (6). We define

$$F = F_0 + F_x + F_y, \quad (\text{S-1a})$$

$$F_0 = T \sum_{\boldsymbol{\varepsilon}} \int \frac{d\mathbf{p}}{(2\pi)^2} \tilde{\gamma}^{-1} \left[\hat{B}_x \hat{B}_x + \hat{B}_y \hat{B}_y \right], \quad (\text{S-1b})$$

$$F_x = -\frac{1}{2} T \sum_{\boldsymbol{\varepsilon}} \int \frac{d\mathbf{p}}{(2\pi)^2} \text{Tr} \ln \left(g_{0x}^{-1} - \hat{b}_{1x} - \hat{b}_{2x} \right), \quad (\text{S-1c})$$

$$F_y = -\frac{1}{2} T \sum_{\boldsymbol{\varepsilon}} \int \frac{d\mathbf{p}}{(2\pi)^2} \text{Tr} \ln \left(g_{0y}^{-1} - \hat{b}_{1y} - \hat{b}_{2y} \right). \quad (\text{S-1d})$$

We use the formula

$$\det(M) = \det B \det(A - DB^{-1}C), \quad \text{for all } M = \begin{pmatrix} A & D \\ C & B \end{pmatrix}, \quad (\text{S-2})$$

where A, B, C, D are matrices. We reduce the free energy in the direction Σ_x ,

$$\begin{aligned} M_x &= i\varepsilon + (\hat{\mathbf{v}}\mathbf{p})_{\Sigma_x} - b_{1x}\Lambda_2 - b_{2x}L_2\Lambda_3 \\ &= \begin{pmatrix} M_1^a & ib_{2x}\Lambda_3 \\ -ib_{2x}\Lambda_3 & M_1^b \end{pmatrix}_L, \end{aligned} \quad (\text{S-3})$$

with

$$M_1^a = i\varepsilon + vp_x \cos \theta \Lambda_3 + vp_y \sin \theta \Lambda_3 - b_{1x}\Lambda_2, \quad (\text{S-4a})$$

$$M_1^b = i\varepsilon - vp_x \cos \theta \Lambda_3 + vp_y \sin \theta \Lambda_3 - b_{1x}\Lambda_2, \quad (\text{S-4b})$$

which leads to

$$\det M = \det M_1^b \det M_1, \quad (\text{S-5a})$$

$$M_1 = M_1^a - b_{2x}^2 \Lambda_3 \left(M_1^b \right)^{-1} \Lambda_3. \quad (\text{S-5b})$$

We now decompose once again with

$$M_1 = (i\varepsilon - b_{1x}\Lambda_2 + vp_x \cos \theta \Lambda_3) (1 + \bar{d}_2) + vp_y \sin \theta \Lambda_3 (1 - \bar{d}_2), \quad (\text{S-6a})$$

$$\bar{d}_2 = \frac{b_{2x}^2}{\varepsilon^2 + (vp_x \cos \theta - vp_y \sin \theta)^2 + b_{1x}^2}, \quad (\text{S-6b})$$

$$M_1 = \begin{pmatrix} M_2^a & ib_{1x}(1 + \bar{d}_2) \\ -ib_{1x}(1 + \bar{d}_2) & M_2^b \end{pmatrix}_{\Lambda}, \quad \text{with} \quad (\text{S-6c})$$

$$M_2^a = (i\varepsilon + vp_x \cos \theta) (1 + \bar{d}_2) + vp_y \sin \theta (1 - \bar{d}_2), \quad (\text{S-6d})$$

$$M_2^b = (i\varepsilon - vp_x \cos \theta) (1 + \bar{d}_2) - vp_y \sin \theta (1 - \bar{d}_2). \quad (\text{S-6e})$$

We get

$$\det M_x = \det M_1^b \det M_2^b \det M_2, \quad (\text{S-7a})$$

$$M_2 = M_2^a - \frac{b_{1x}^2 (1 + \bar{d}_2)^2}{(i\varepsilon - vp_x \cos \theta) (1 + \bar{d}_2) - vp_y \sin \theta (1 + \bar{d}_2)}. \quad (\text{S-7b})$$

We finally obtain

$$\det M_x = \frac{(\varepsilon^2 + b_{1x}^2) d_x^2 + (vp_x \cos \theta d_x + vp_y \sin \theta (d_x - 2b_{2x}^2))^2}{d_x - b_{2x}^2}, \quad (\text{S-8a})$$

$$d_x = \varepsilon^2 + (vp_x \cos \theta - vp_y \sin \theta)^2 + b_{1x}^2 + b_{2x}^2. \quad (\text{S-8b})$$

Reducing in the same manner the projection onto the Σ_y axis, and noticing that we get the right formulae by shifting $\theta \rightarrow \pi/2 - \theta$, we have

$$\det M_y = \frac{(\varepsilon^2 + b_{1y}^2) d_y^2 + (vp_x \sin \theta d_y + vp_y \cos \theta (d_y - 2b_{2y}^2))^2}{d_y - b_{2y}^2}, \quad (\text{S-9a})$$

$$d_y = \varepsilon^2 + (vp_x \sin \theta - vp_y \cos \theta)^2 + b_{1y}^2 + b_{2y}^2, \quad (\text{S-9b})$$

we finally get for the free energy :

$$F = F_0 + F_x + F_y, \quad (\text{S-10a})$$

$$F_0 = T \sum_{\varepsilon} \int \frac{d\mathbf{p}}{(2\pi)^2} \tilde{\gamma}^{-1} [\bar{B}_{1x} B_{1x} + \bar{B}_{1y} B_{1y} + \bar{B}_{2x} B_{2x} + \bar{B}_{2y} B_{2y}], \quad (\text{S-10b})$$

$$F_x = -\frac{1}{2} T \sum_{\varepsilon} \int \frac{d\mathbf{p}}{(2\pi)^2} \left[-\ln(d_x - b_{2x}^2) + \ln \left((\varepsilon^2 + b_{1x}^2) d_x^2 + (vp_x \cos \theta d_x + vp_y \sin \theta (d_x - 2b_{2x}^2))^2 \right) \right], \quad (\text{S-10c})$$

$$F_y = -\frac{1}{2} T \sum_{\varepsilon} \int \frac{d\mathbf{p}}{(2\pi)^2} \left[-\ln(d_y - b_{2y}^2) + \ln \left((\varepsilon^2 + b_{1y}^2) d_y^2 + (vp_x \sin \theta d_y + vp_y \cos \theta (d_y - 2b_{2y}^2))^2 \right) \right], \quad (\text{S-10d})$$

$$b_x = \bar{B}_x + B_y, \quad b_y = \bar{B}_y + B_x. \quad (\text{S-10e})$$

II. MFES

We give below some details about the MFE. They are obtained by differentiating Eqs. (S-10) with respect to $\bar{B}_{x(y)}$ and $B_{x(y)}$ respectively. We get

$$\tilde{\gamma}^{-1} \hat{B}_x = -\frac{1}{2} \text{Tr} [\hat{g}_x], \quad (\text{S-11a})$$

$$\tilde{\gamma}^{-1} \hat{B}_x = -\frac{1}{2} \text{Tr} [\hat{g}_y], \quad (\text{S-11b})$$

$$\tilde{\gamma}^{-1} \hat{B}_y = -\frac{1}{2} \text{Tr} [\hat{g}_y], \quad (\text{S-11c})$$

$$\tilde{\gamma}^{-1} \hat{B}_y = -\frac{1}{2} \text{Tr} [\hat{g}_x], \quad (\text{S-11d})$$

$$\hat{g}_x = (g_{0x}^{-1} + \hat{b}_x)^{-1}, \quad \hat{g}_y = (g_{0y}^{-1} + \hat{b}_y)^{-1}. \quad (\text{S-11e})$$

We see that when the MFE do have a solution, Eq. (S-11a) reduces identically to Eq. (S-11d) and Eq. (S-11b) reduces to Eq. (S-11c). Two constraints are naturally obtained :

$$\hat{B}_x = \hat{B}_y, \quad \hat{B}_y = \hat{B}_x. \quad (\text{S-12})$$

The constraints (S-12) correspond to a condition of reality for the fields $\hat{B}_{x(y)}$ within the conjugation operation introduced in (4).

We proceed by differentiating Eq. (S-10) with respect to $b_{1x}, b_{1y}, b_{2x}, b_{2y}$ to get the gap equations ;

$$\gamma_0^{-1} B_{1x} = -T \sum_{\epsilon} \int \frac{d\mathbf{p}}{(2\pi)^2} \hat{D} \frac{\partial F_x}{\partial b_{1x}}, \quad (\text{S-13a})$$

$$\gamma_0^{-1} B_{1y} = -T \sum_{\epsilon} \int \frac{d\mathbf{p}}{(2\pi)^2} \hat{D} \frac{\partial F_y}{\partial b_{1y}}, \quad (\text{S-13b})$$

$$\gamma_1^{-1} B_{2x} = -T \sum_{\epsilon} \int \frac{d\mathbf{p}}{(2\pi)^2} \hat{D} \frac{\partial F_x}{\partial b_{2x}}, \quad (\text{S-13c})$$

$$\gamma_1^{-1} B_{2y} = -T \sum_{\epsilon} \int \frac{d\mathbf{p}}{(2\pi)^2} \hat{D} \frac{\partial F_y}{\partial b_{2y}}, \quad (\text{S-13d})$$

$$\gamma_0 = \frac{3g^2}{2}, \quad \gamma_1 = \frac{3g_1^2}{2}. \quad (\text{S-13e})$$

It is useful to introduce the notations ($x_1 = b_{1x}^2, x_2 = b_{2x}^2, y_1 = b_{1y}^2, y_2 = b_{2y}^2$)

$$A_{1x} = - \int \frac{d\mathbf{p}}{(2\pi)^2} \hat{D} \frac{\partial F_x}{\partial x_1}, \quad (\text{S-14a})$$

$$A_{2x} = - \int \frac{d\mathbf{p}}{(2\pi)^2} \hat{D} \frac{\partial F_x}{\partial x_2}, \quad (\text{S-14b})$$

$$A_{1y} = - \int \frac{d\mathbf{p}}{(2\pi)^2} \hat{D} \frac{\partial F_y}{\partial y_1}, \quad (\text{S-14c})$$

$$A_{2y} = - \int \frac{d\mathbf{p}}{(2\pi)^2} \hat{D} \frac{\partial F_y}{\partial y_2}. \quad (\text{S-14d})$$

The expressions for the partial derivatives are given in Eq. (8). With these notations, the MFE write

$$\gamma_0^{-1} B_{1x} = -2T \sum_{\epsilon} b_{1x} A_{1x}, \quad (\text{S-15a})$$

$$\gamma_0^{-1} B_{1y} = -2T \sum_{\epsilon} b_{1y} A_{1y}, \quad (\text{S-15b})$$

$$\gamma_1^{-1} B_{2x} = -2T \sum_{\epsilon} b_{2x} A_{2x}, \quad (\text{S-15c})$$

$$\gamma_1^{-1} B_{2y} = -2T \sum_{\epsilon} b_{2y} A_{2y}. \quad (\text{S-15d})$$

III. STRUCTURE OF THE MF SOLUTIONS

In Fig.2 are depicted the typical form of the QDW/SC and CDW components of the CE solution. Despite the CE solution, the MFEs (7a-7d) admits two other solutions that we describe here.

The pure QDW/SC solution is depicted on Fig. 6 below. The most noticeable fact about this solution is the very feeble dependence on the Fermi velocity angle θ . This solution is very robust to changes of the shape of the Fermi surface at the hot-spots and at the anti-nodes, characterized by $\theta = 0$ for flat portions of the Fermi surface at the anti-nodes and $\theta = \pi/4$ for the generic case. The pure QDW/SC solution is very similar to the observed PG of cuprate superconductors in that respect.

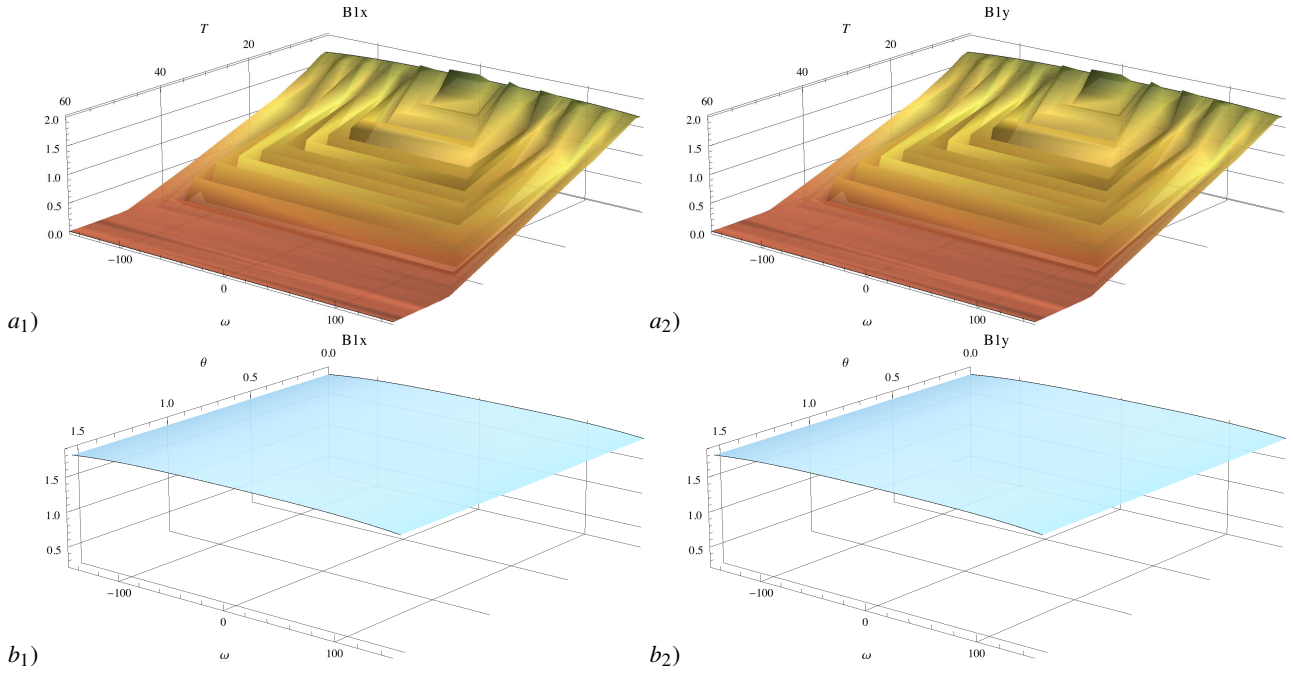


FIG. 6. (Color online) Typical solution for the pure QDW/SC solution, as a function of (ϵ_n, T) for $a_1)$ and $a_2)$, and as a function of (ϵ_n, θ) for $b_1)$ and $b_2)$. The values of the parameters are $g = 20$, $g_1 = 30$, $v = 6$, $m_a = 0.1$, $\gamma = 3$, $W = 2\pi$. The velocity angle is $\theta = 0.1$ for $a_1)$ and $a_2)$ whereas the temperature is $T = 1$ for $b_1)$ and $b_2)$. Note the very feeble dependence in the Fermi angle for this solution.

In contrast, the pure CDW solution depicted in Fig.7 show that the pure CDW solution is much more dependent on the angle θ of the Fermi velocity at the anti-nodes.

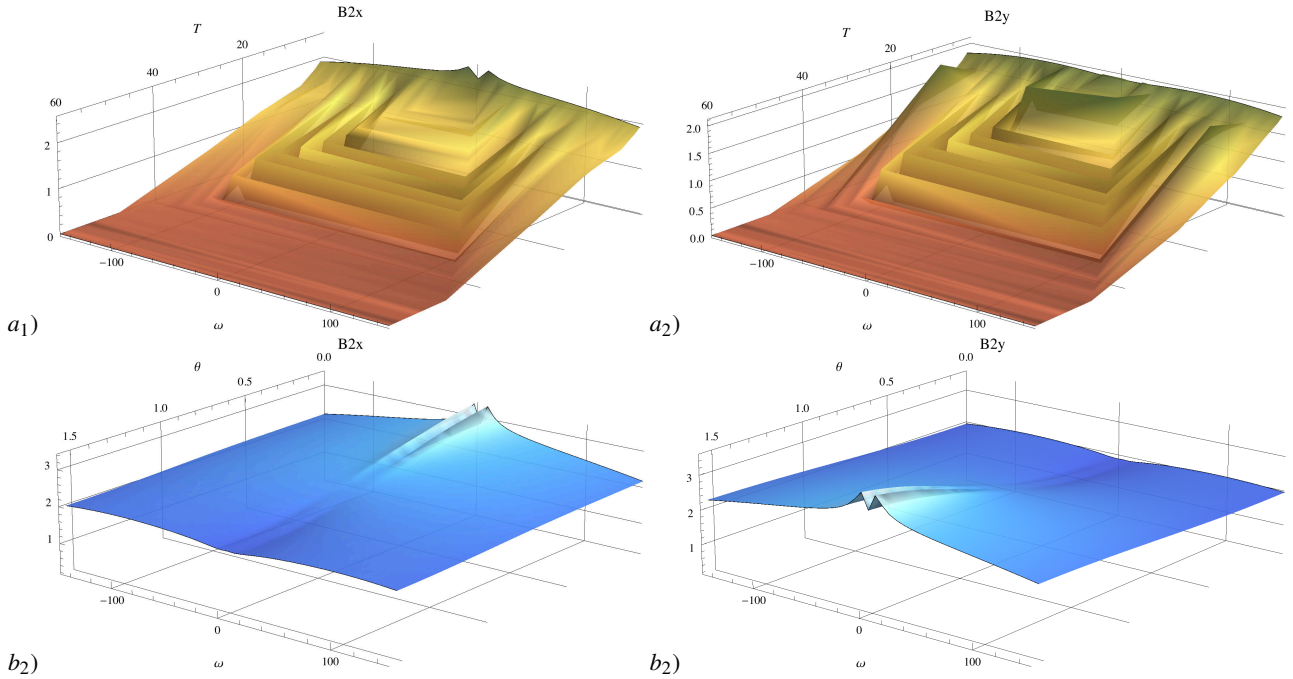


FIG. 7. (Color online) Typical solution for the pure CDW solution, as a function of (ϵ_n, T) for $a_1)$ and $a_2)$, and as a function of (ϵ_n, θ) for $b_1)$ and $b_2)$. The values of the parameters are $g = 20$, $g_1 = 30$, $v = 6$, $m_a = 0.1$, $\gamma = 3$, $W = 2\pi$. The velocity angle is $\theta = 0.1$ for $a_1)$ and $a_2)$ whereas the temperature is $T = 1$ for $b_1)$ and $b_2)$. Note that although the T -dependence of the solution is different from the one on Fig.7, especially as the magnitude of the solution is concerned, its angular dependence is very similar to the one depicted in Fig.7.

IV. FLUCTUATIONS

We expand below the free energy at the order two in order to find the stability condition (11) and to evaluate the factors δA_i . Let us derive the stability condition for one order parameter b_x, b_y . Noting $x = b_x^2$ and $y = b_y^2$, we have

$$F = F_0 + F_x(x) + F_y(y). \quad (\text{S-16})$$

Using $B = B_0 + \delta B$ and $\bar{B} = \bar{B}_0 + \delta \bar{B}$ we get

$$F_0 = F_0^{(0)} + F_0^{(1)} + F_0^{(2)}, \quad (\text{S-17a})$$

$$F_0^{(1)} = \gamma^{-1} (\bar{B}_{x0} \delta B_x + B_{x0} \delta \bar{B}_x + \bar{B}_{y0} \delta B_y + B_{y0} \delta \bar{B}_{y0}), \quad (\text{S-17b})$$

$$F_0^{(2)} = \gamma^{-1} (\delta \bar{B}_x \delta B_x + \delta \bar{B}_y \delta B_y). \quad (\text{S-17c})$$

From the MF relations $\bar{B}_{x0} = B_{y0}$ and $\bar{B}_{y0} = B_{x0}$ we obtain

$$F_0^{(1)} = \gamma^{-1} (B_{x0} \delta b_x + B_{y0} \delta b_y), \quad (\text{S-18a})$$

$$\delta b_x = \delta \bar{B}_x + \delta B_y, \quad (\text{S-18b})$$

$$\delta b_y = \delta \bar{B}_y + \delta B_x. \quad (\text{S-18c})$$

Now let us consider the second term in the Free energy:

$$F_x^{(1)} = 2b_{x0} F_x' \delta b_x, \quad (\text{S-19a})$$

$$F_x^{(2)} = (F_x' + 2b_{x0}^2 F_x'') (\delta b_x)^2, \quad (\text{S-19b})$$

$$F_y^{(1)} = 2b_{y0} F_y' \delta b_y, \quad (\text{S-19c})$$

$$F_y^{(2)} = (F_y' + 2b_{y0}^2 F_y'') (\delta b_y)^2. \quad (\text{S-19d})$$

Hence we get for the factors δA_i (notation: $x_1 = b_{1x}^2, x_2 = b_{2x}^2, y_1 = b_{1y}^2, y_2 = b_{2y}^2$)

$$\delta A_{1x} = 2 \int \frac{d\mathbf{q}}{(2\pi)^2} D(\omega, \mathbf{q}) b_{1x}^2 \frac{\partial^2 F}{\partial x_1^2}, \quad (\text{S-20a})$$

$$\delta A_{2x} = 2 \int \frac{d\mathbf{q}}{(2\pi)^2} D(\omega, \mathbf{q}) b_{2x}^2 \frac{\partial^2 F}{\partial x_2^2}, \quad (\text{S-20b})$$

$$\delta A_{1y} = 2 \int \frac{d\mathbf{q}}{(2\pi)^2} D(\omega, \mathbf{q}) b_{1y}^2 \frac{\partial^2 F}{\partial y_1^2}, \quad (\text{S-20c})$$

$$\delta A_{2y} = 2 \int \frac{d\mathbf{q}}{(2\pi)^2} D(\omega, \mathbf{q}) b_{2y}^2 \frac{\partial^2 F}{\partial y_2^2}, \quad (\text{S-20d})$$

with

$$\frac{\partial^2 F}{\partial x_1^2} = \frac{d_{numx1}}{d_{denx}}, \quad (\text{S-21a})$$

$$d_{denx} = (d_x^2 + 4vq_x vq_y \cos \theta \sin \theta d_x - 4b_{2x}^2 v^2 q_y^2 \sin^2 \theta)^2, \quad (\text{S-21b})$$

$$d_{numx1} = d_x^2 + 4vq_x vq_y \cos \theta \sin \theta (d_x + 2vq_x vq_y \cos \theta \sin \theta) + 2b_{2x}^2 v^2 q_y^2 \sin^2 \theta, \quad (\text{S-21c})$$

and

$$\frac{\partial^2 F}{\partial y_1^2} = \frac{d_{numy1}}{d_{deny}}, \quad (\text{S-22a})$$

$$d_{deny} = (d_y^2 + 4vq_x vq_y \cos \theta \sin \theta d_y - 4b_{2y}^2 v^2 q_x^2 \cos^2 \theta)^2, \quad (\text{S-22b})$$

$$d_{numy1} = d_y^2 + 4vq_x vq_y \cos \theta \sin \theta (d_y + 2vq_x vq_y \cos \theta \sin \theta) + 2b_{2y}^2 v^2 q_x^2 \cos^2 \theta, \quad (\text{S-22c})$$

and

$$\frac{\partial^2 F}{\partial x_2^2} = \frac{d_{numx2}}{d_{denx}}, \quad (\text{S-23a})$$

$$d_{denx} = (d_x^2 + 4vq_x vq_y \cos \theta \sin \theta d_x - 4b_{2x}^2 v^2 q_y^2 \sin^2 \theta)^2, \quad (\text{S-23b})$$

$$d_{numx2} = d_x^2 + 4vq_x vq_y \cos \theta \sin \theta d_x - 4b_{2x}^2 v^2 q_y^2 \sin^2 \theta (2b_{1x}^2 + 2\varepsilon^2 + b_{2x}^2), \quad (\text{S-23c})$$

and

$$\frac{\partial^2 F}{\partial y_2^2} = \frac{d_{numy2}}{d_{deny}}, \quad (\text{S-24a})$$

$$d_{deny} = (d_y^2 + 4vq_x vq_y \cos \theta \sin \theta d_y - 4b_{2y}^2 v^2 q_x^2 \cos^2 \theta)^2, \quad (\text{S-24b})$$

$$d_{numy2} = d_y^2 + 4vq_x vq_y \cos \theta \sin \theta d_y - 4b_{2y}^2 v^2 q_x^2 \cos^2 \theta (2b_{1y}^2 + 2\varepsilon^2 + b_{2y}^2). \quad (\text{S-24c})$$

V. EXTREME LIMIT WHERE $\gamma_1 \gg \gamma_0$ IN EQS. (7a-7d)

Recently, an interesting work [54] has proposed the pure CDW solution as a candidate for the PG phase. This solution is pre-empted by the formation of a $q = 0$ -bond state at the PG temperature T^* , which has the property to give a non zero Kerr signal [30]. It is interesting to see what happens within the study of co-existence when the quadratic coupling constant γ_1 favoring the CDW order is pushed to a very high limit compared to γ_0 . This study is presented below for $\gamma_1 = 10 \gamma_0$.

First, it is worth noticing that the three solutions [pure CDW, pure QDW/SC and the CE solution] are still present in the extreme limit where $\gamma_1 \gg \gamma_0$, which extremely favors the pure CDW order. In this limit as well, the pure CDW solution becomes unstable towards the CE solution. Comparison of the free energies shows that the CE solution has a slightly lower energy than the pure CDW solution in this case, while the splitting with the QDW/SC solution is higher (Fig. 14).

A. MF solutions

We start with the pure CDW solution depicted in Fig. 8. One can observe the large magnitude of the pure CDW solution [graphs a_1) and a_2)] whereas the θ -dependence of the solution [graphs b_1) and b_2)] has not changed compared to the one in Fig. 7.

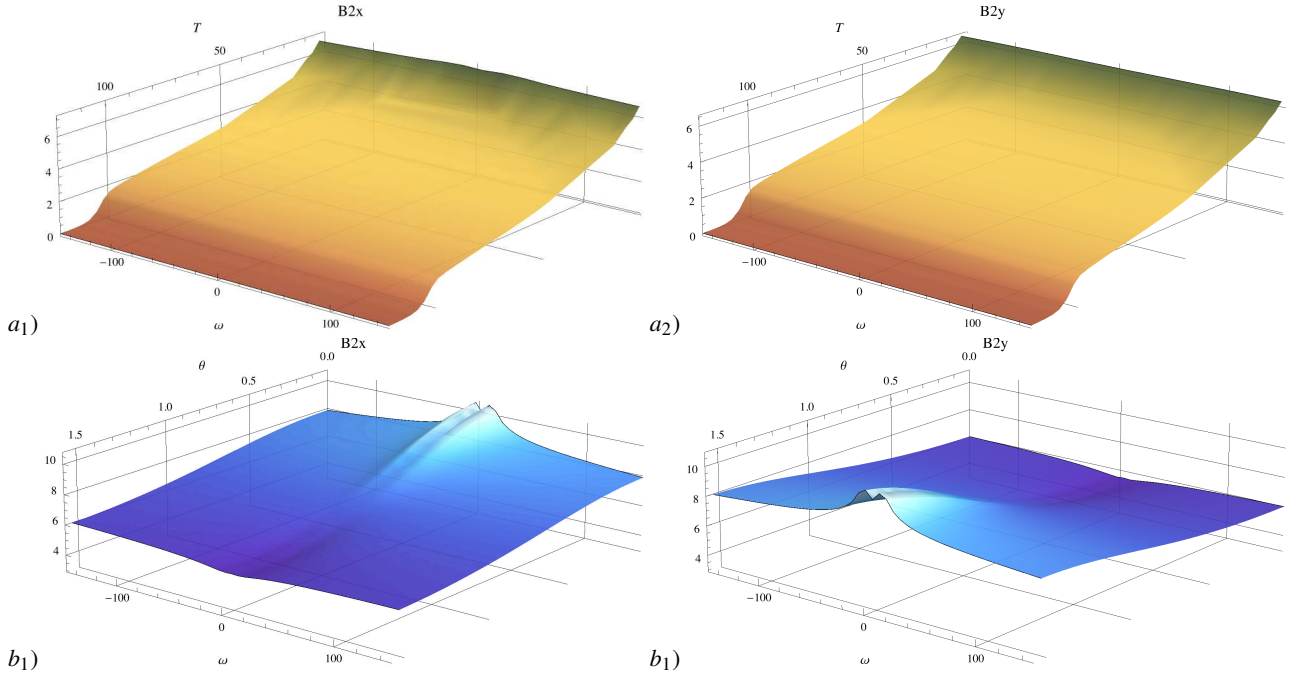


FIG. 8. (Color online) Typical solution for the pure CDW solution, as a function of (ϵ_n, T) for a_1) and a_2), and as a function of (ϵ_n, θ) for b_1) and b_2). The values of the parameters are $g = 20$, $g_1 = 200$, $v = 6$, $m_a = 0.1$, $\gamma = 3$, $W = 2\pi$. The velocity angle is $\theta = 0.1$ for a_1) and a_2) whereas the temperature is $T = 1$ for b_1) and b_2). Note the strong dependence in the Fermi angle for this solution.

We turn now to the pure QDW/SC solution, which was introduced in Ref. [52] as a good candidate for the PG at T^* . Comparing Fig.9 to Fig.6, we see the similarity between the two solutions. It is to be expected since only the parameter γ_1 has been increased between the two figures and the pure QDW/SC solution is insensitive to the value of γ_1 .

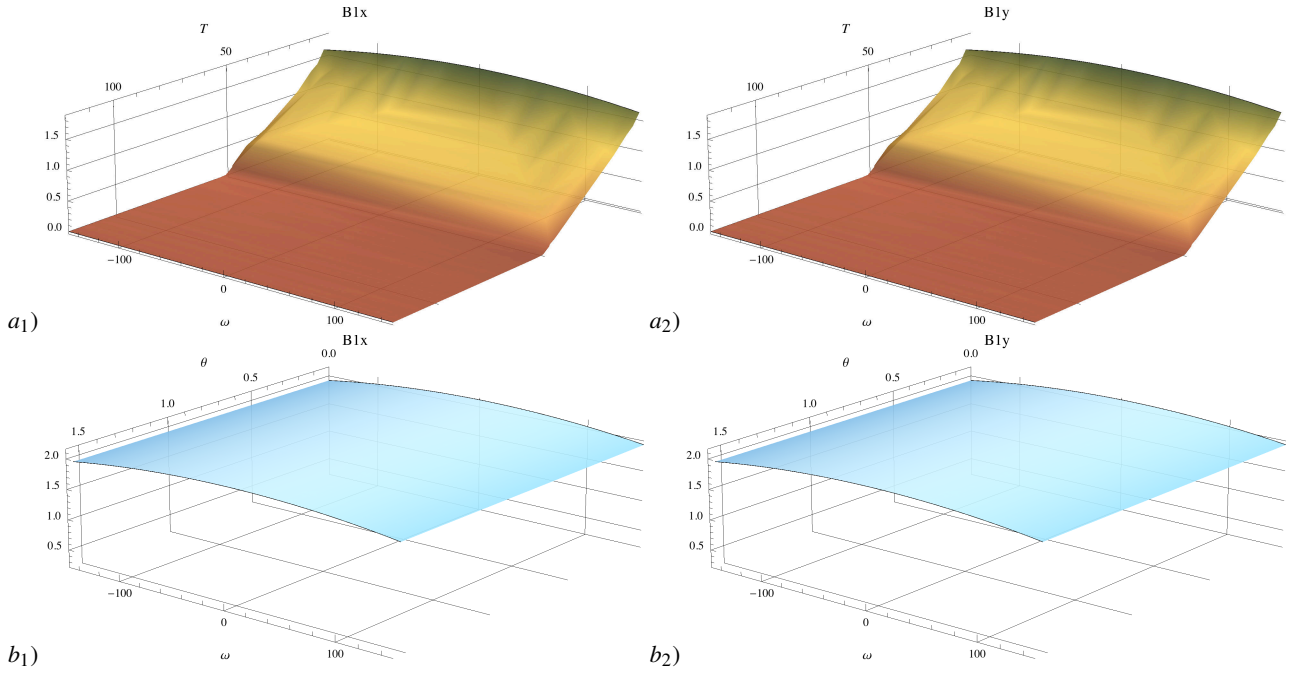
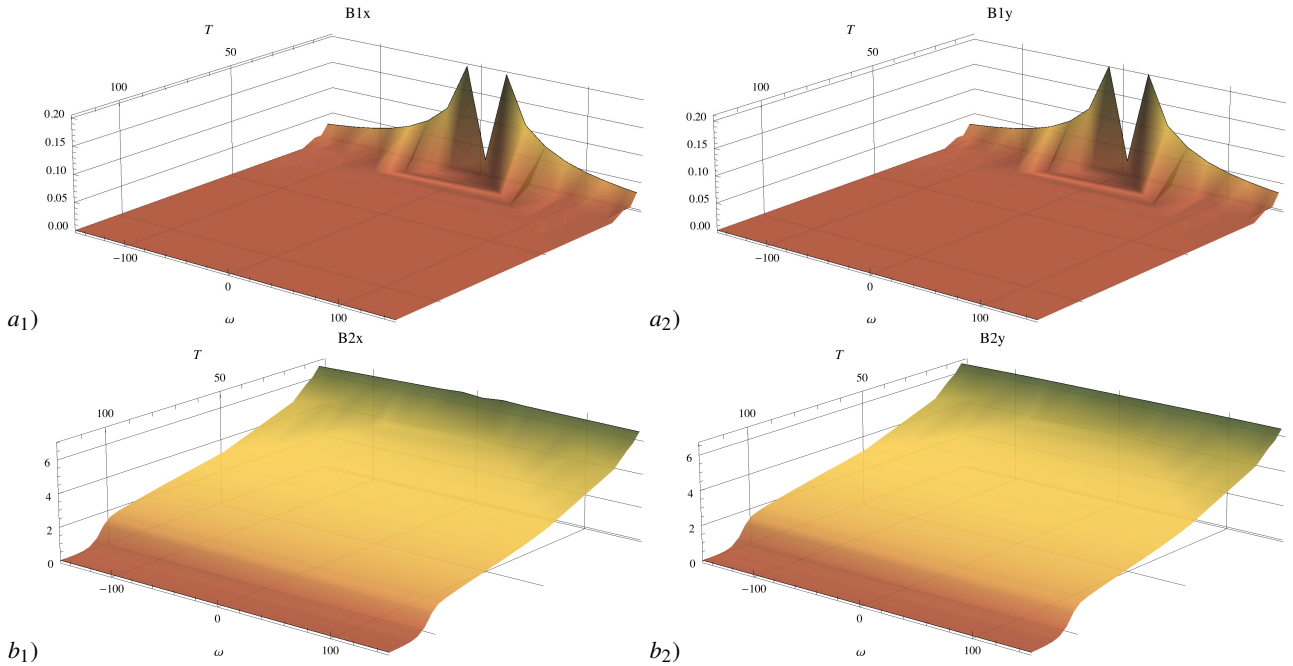


FIG. 9. (Color online) Typical solution for the pure QDW/SC solution, as a function of (ϵ_n, T) for $a_1)$ and $a_2)$, and as a function of (ϵ_n, θ) for $b_1)$ and $b_2)$. The values of the parameters are $g = 20$, $g_1 = 200$, $v = 6$, $m_a = 0.1$, $\gamma = 3$, $W = 2\pi$. The velocity angle is $\theta = 0.1$ for $a_1)$ and $a_2)$ whereas the temperature is $T = 1$ for $b_1)$ and $b_2)$. Note the striking similarities between this solution and the one in Fig.6.

The CE solution is depicted in Fig.10. The trend has been inverted compared to Fig.2. Here the CDW component of the solution [$b_1)$ and $b_2)$ in Fig.10] is one order of magnitude larger than the pure QDW/SC component [$a_1)$ and $a_2)$], in proportion to γ_1/γ_0 . One can also note the pronounced θ -dependence of the QDW/SC solution [$c_1)$ and $c_2)$] compared to the CDW component [$d_1)$ and $d_2)$]. This seems to confirm the intuition of Ref.[54] that it is possible to stabilize the CDW solution compared to the pure QDW/SC solution. The price to be paid however is to enforce $\gamma_1 \gg \gamma_0$ to such an extent that seems a bit artificial for high T_c -cuprates. Moreover even when a giant CDW solution is stabilized, we observed a re-entrance of the QDW/SC component at lower temperatures. The conclusion is that it is very difficult to get rid totally of the QDW/SC component.



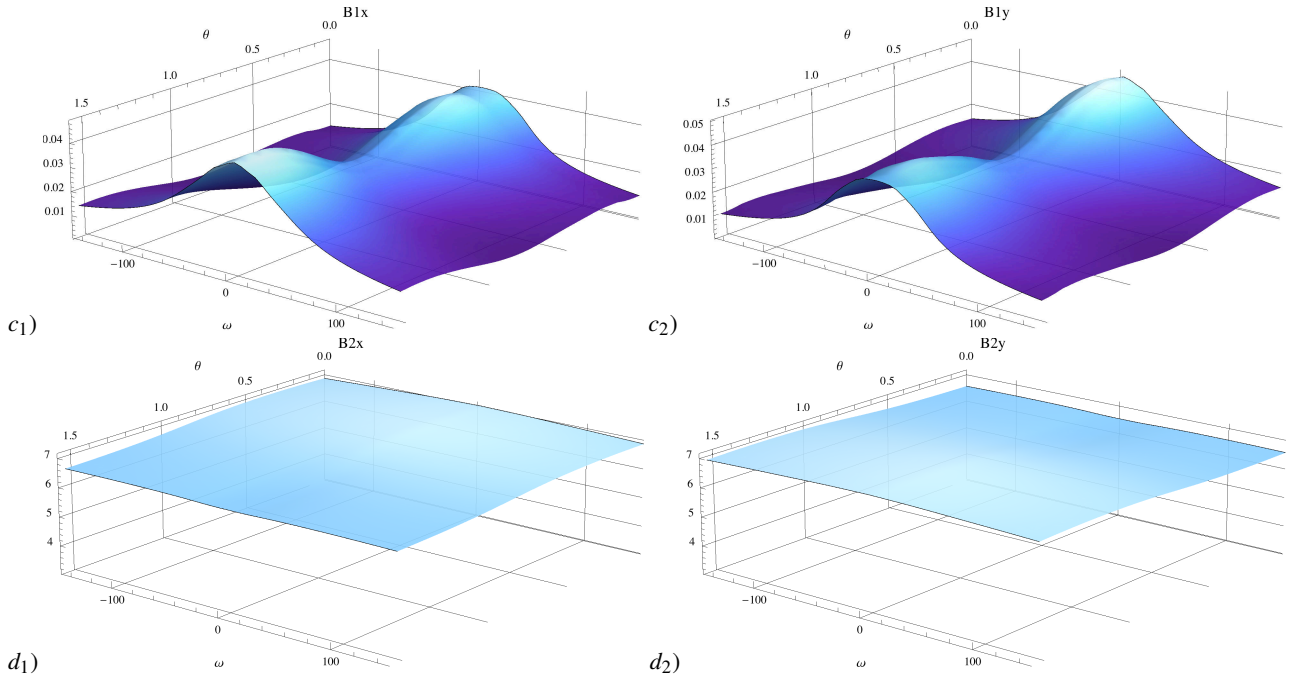


FIG. 10. (Color online) Typical solutions for the QDW/SC ($B_{1x,y}$) and CDW ($B_{2x,y}$) in the CE phase. The values of the parameters are $g = 20$, $g_1 = 200$, $v = 6$, $m_a = 0.1$, $\gamma = 3$, $W = 2\pi$. The velocity angle is $\theta = 0.1$ for a_1 , a_2 , b_1 and b_2) whereas the temperature is $T = 1$ for c_1 , c_2 , d_1) and d_2). Note the contrast with the CE solution of Fig.2. Here the CDW component is one order of magnitude larger than the QDW/SC component and the θ dependence of the CDW component [d_1) and d_2)] is minimal compared to the one of the QDW/SC component [c_1) and c_2)].

B. Stability conditions

We give now the stability conditions for the various solution in the limit $\gamma_1 \gg \gamma_0$, in analogy with Fig.4. The results of this investigation are quite unexpected. Although the limit $\gamma_1 \gg \gamma_0$ is extremely favorable to the pure CDW solution, we can see that at low temperatures (here the study is made at $T = 1K$) this solution becomes unstable in the direction of the QDW/SC [dir. B_1 in these notations], indicating an instability towards co-existence at low temperature. This observation corroborates the results of section III where it was concluded that it is very difficult to get rid completely of the QDW/SC solution. Notice that the pure QDW/SC solution (Fig. 11) is now stable in one direction but becomes unstable in the direction of the CDW solution, due to the favorable ratio $\gamma_1/\gamma_0 \gg 1$. Lastly, the CE solution becomes stable in the two directions (Fig. 13).

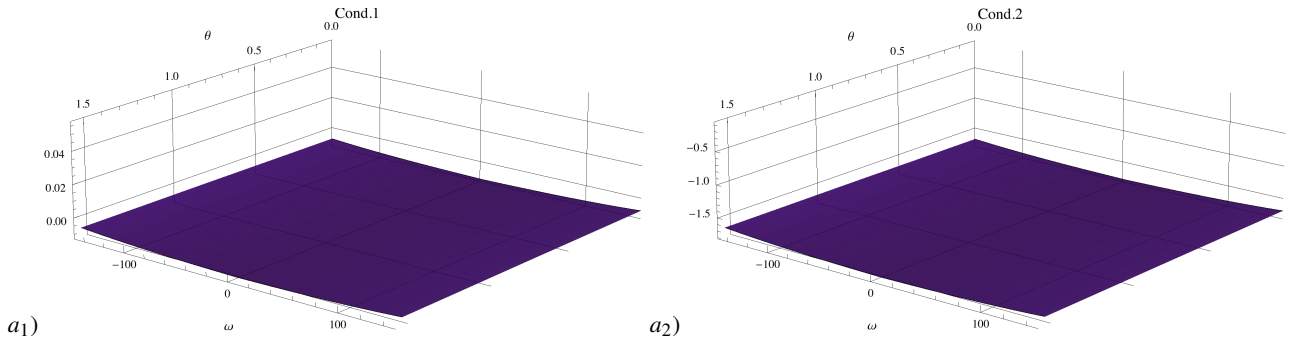


FIG. 11. (Color online) Stability conditions (11) for the pure QDW/SC solution as a function of (ϵ_n, θ) for $T = 1K$. a_1) [dir. B_1] and a_2) [dir. B_2]. Note that although the limit $\gamma_1 \gg \gamma_0$ is very defavorable to this solution, it is still stable.

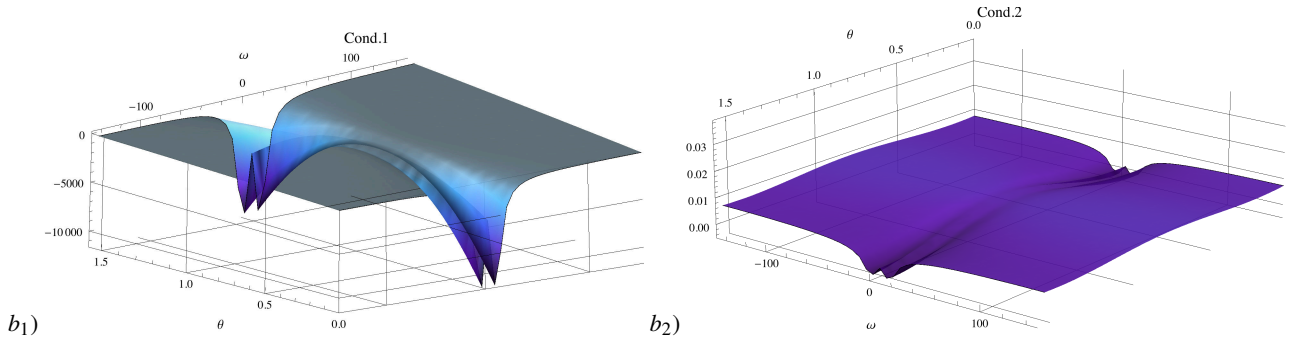


FIG. 12. (Color online) Stability conditions (11) for the pure CDW solution as a function of (ε_n, θ) for $T = 1K$. a_1) [dir. B_1] and a_2) [dir. B_2]. Note that although the limit $\gamma_1 \gg \gamma_0$ is energetically very favorable to this solution, there is a direction of instability [dir. B_1] at low temperature, indicating an instability towards the CE solution.

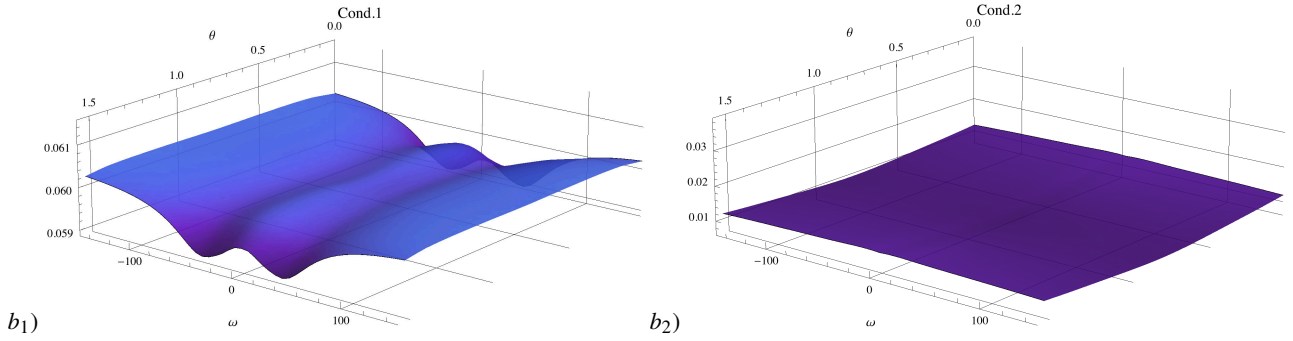


FIG. 13. (Color online) Stability conditions (11) for the pure CE solution as a function of (ε_n, θ) for $T = 1K$. a_1) [dir. B_1] and a_2) [dir. B_2]. Note that the CE solution is stable in both directions at low temperatures.

C. Free energy

Lastly we turn to the comparison of the free energy for the three solution in the limit $\gamma_1 \gg \gamma_2$. The result is shown in Fig.14. By comparison with Fig.5 we see that the energy of the pure QDW/SC solution is now higher than the one of the pure CDW solution. The co-existence solution, however, is always the lowest one, although quite close in energy to the pure CDW solution. This gives support to our conclusion that the system is in fine unstable towards the CE solution.

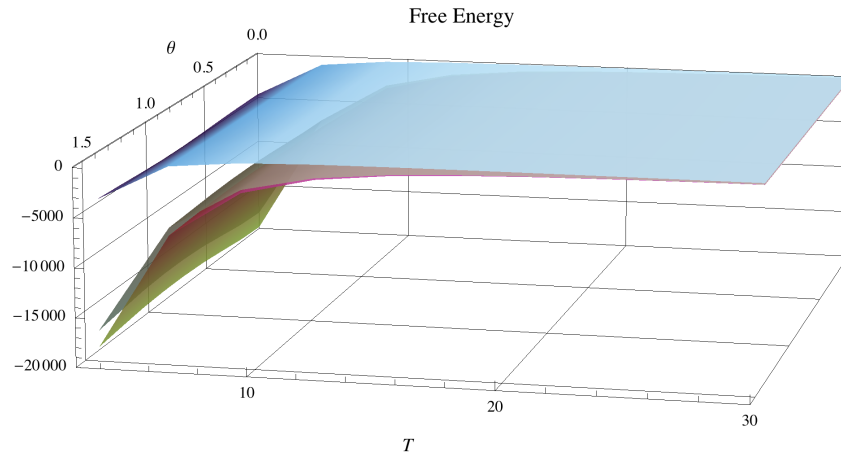


FIG. 14. (Color online) Free energy at of the three MF solutions. Pure CDW (brown), pure QDW/SC (dark blue) and CE (neon colors). The values of the parameters are $g = 20$, $g_1 = 200$, $\nu = 6$, $m_a = 0.1$, $\gamma = 3$, $W = 2\pi$ and $\theta = 0.1$.